Experimental Approach to Selection of Pulsing Parameters in Pulsed GMAW

A method for selection of process parameters in pulsed GMAW helps to efficiently develop welding procedures

BY S. SUBRAMANIAM, D. R. WHITE, J. E. JONES AND D. W. LYONS

ABSTRACT. An efficient method of identifying power supply pulsing parameters for pulsed gas metal arc welding based on statistical experimental design is presented. Fractional factorial screening experiments are combined with D-optimal experimental designs to allow the user to develop an accurate wire feed rate model for varying pulsing conditions and to characterize the desirable one droplet per pulse (ODPP) operating region for a given wire type and diameter. Equations defining the wire feed rates and time at a given peak current required for ODPP transfer are presented. Compared to conventional techniques, a very small number of experiments is required. A power-supply-dependent approach and a more generic method employing measured rather than nominal current values are presented. Joints produced using this approach are evaluated and found to meet applicable bead geometry standards.

Introduction

Identifying suitable combinations of welding parameters for use with pulsed gas metal arc welding (GMAW-P) can be a time-consuming process, involving considerable trial and error. The primary parameters to be identified are wire feed rate, peak current, background current, duty cycle and pulsing frequency. As illustrated in Fig. 1, the welding parameters are more numerous than in conventional GMAW, and the process is typically more sensitive to parameter changes. As a result, careful parameter selection is important. To address this, "synergic" pulsed GMAW power supplies are commonly used in industry (Refs. 1, 2). In these systems, the relationship between a digitally controlled wire feed rate and the pulsing parameters is managed by microprocessor-based look-up tables. While easy to use, these systems do not give the user much flexibility. Thus, they are limited in their capabilities for special applications such as very thin sections or very high speed.

In addition to operating in the synergic mode, in which the user typically selects only the material (*i.e.*, steel, aluminum, stainless steel) to be welded and a power level, many modern power supplies also allow users to select pulsing parameters. However, the task of determining what the welding parameters should be can be very time consuming and experimentally intensive, as evidenced by product literature for some synergic power supplies, which notes that millions of experiments were conducted to determine optimum power supply settings for various applications (Ref. 3). No efficient method has been described in the open scientific literature for establishing viable pulsing parameters in GMAW-P. Efficient use of statistical design of experiments (DOE) techniques, such as fractional factorial design and D-optimal design, allows development of an empirical methodology, incorporating a scientific approach to welding procedure development. The D-optimal design technique, with its flexibility in defining the experimental space, is useful for modeling the nonlinear aspects of arc welding processes. This is not easy to do with conventional experimental design techniques where requirements for orthogonality may make it more difficult to characterize the process. The purpose of this paper is to present an experimental methodology for identifying and optimizing certain characteristics of weld pulsing parameters.

KEY WORDS

Fractional Factorial
D-Optimal
Pulsing
GMAW-P
Droplet Transfer
Peak Current
Background Current
Gas Metal Arc

Background

Salter and Doherty (Ref. 4) identified the operating boundary for submerged arc welding and GTA welding experimentally using design of experiments. They developed empirical relations for bead geometry parameters and suggested that empirical equations can be used to pick robust solutions or welding procedures, so that the visual quality acceptance criteria are satisfied when the weld process inputs vary between given levels.

Several other researchers have used factorial techniques to identify the effects of main factors and their interactions in controlling weld quality. The experimental results are used to develop regression

S. SUBRAMANIAM and D. R. WHITE are with Ford Research Laboratory, Dearborn, Mich. J. E. JONES is with N.A. Technologies, Golden, Colo. D. W. LYONS is with Department of Mechanical and Aerospace Engineering, West Virginia University, Morgantown, W.Va.

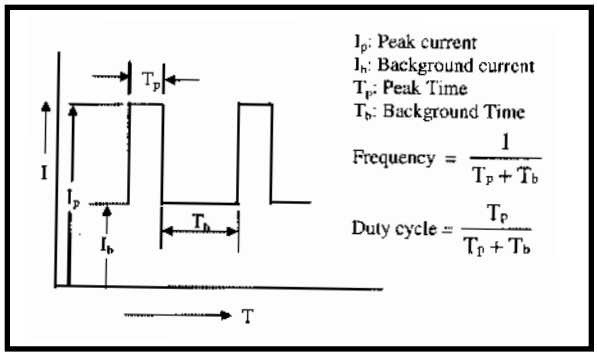

Fig. 1 — Current waveform for pulsed GMA welding.

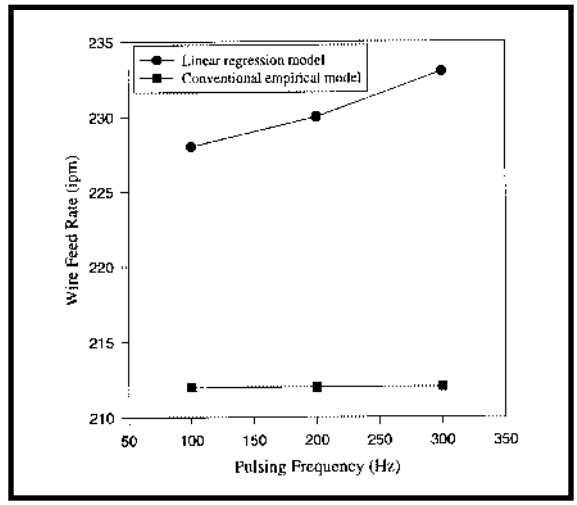

Fig. 2 — Comparison of conventional empirical and linear wire feed rate models. (I_p = 320 A, I_b = 70 A, D: 20%, L = 25 mm.)

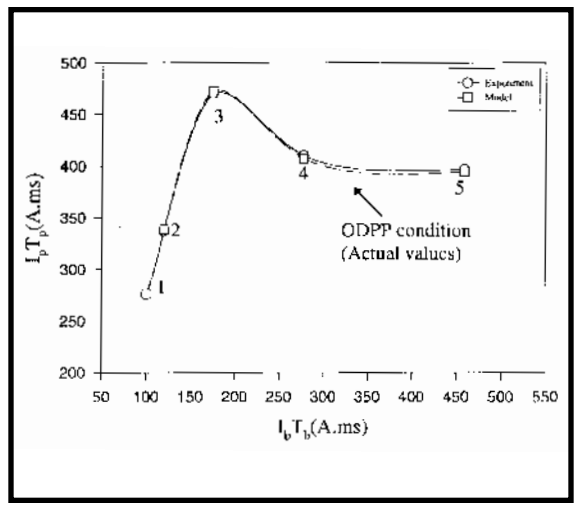

Fig. 3 — Relation between peak and background conditions for ODPP using continuously measured values of I_p and I_b shown in Table 4.

models of the process. The regression equations can be used to select robust welding procedures and set tolerance limits on the welding parameters, given some requirement for weld bead geometry. This can be done by incorporating the equations in a simple computer program (Refs. 5–10).

Amin (Ref. 11) presented a method for defining pulsing parameters in which a simple linear model is first developed to define wire feed rate as a function of mean current, using experimental data. The limiting pulsing parameters are then defined from power law models of the type $I^a_pT_p$=b, where I_p is peak current, T_p is peak time and a and b are constants, for condition of one droplet per pulse. Other researchers have also developed power law models based on observations of droplet detachment using high-speed filming or analysis of signals (Refs. 12–19).

In this work, one objective was to minimize experimentation required to define pulsing parameters when welding over a wide range of travel speeds and plate thicknesses. It was therefore necessary to determine appropriate wire feed rates and pulsing parameters in GMAW-P processes using a relatively small number of experiments. The approach developed applies factorial and optimal experimental design techniques and modeling tools to analyze the process, reducing trial and error involved in procedure development.

This approach has five steps that are described in detail in this paper.

- Conduct screening experiments.
- Develop a wire feed rate model to establish a stable operating region.
- Use D-optimal experimental design to characterize the operable welding region with a minimum number of experiments.
- Characterize the one droplet per pulse (ODPP) region.
- Select welding parameters optimized for the application.

Experimental Equipment

All welding was carried out using a Miller Maxtron 450 welding power supply in the constant current mode. The power supply was controlled using a commercially available controller (Ref. 20) to program the pulse parameters over a wide range. A 4047 aluminum alloy welding wire with a diameter of 1.2 mm was used in the experiments. Argon shielding gas was supplied at a flow rate of 30 ft^3/h. Lap joints were made on Alcoa alloys C210-T6 (6963-T6) extrusions and C119-T6 castings.

High-speed filming at 2000 frames per second was used to characterize the metal transfer behavior. Experiments were carried out using a laser shadowgraph system. In this method, as described in detail by Allemand, *et al.* (Ref. 21), a He-Ne laser acts as a backlight and is passed through a set of lenses and filters. In the process, almost all of the arc light is eliminated and a shadow of the drop and the wire is captured by a high-speed camera.

During welding, the current and voltage signals were recorded using a Nicolet digital oscilloscope at a rate of 50 kHz in order to detect droplet detachments, which were verified with high-speed films. Noise in the process signals was removed using a 5-kHz low-pass filter. Following filtering, it is possible to detect droplet detachments during welding by looking at the small spikes in the voltage signal (Ref. 22). The current and voltage values were recorded and used to calculate the actual values of I_pT_p, I_bT_b (where I_p is peak current, I_b is background current, T_p is peak time, T_b is background time), average current and the power inputs.

The values I_pT_p and I_bT_b were calculated from the area under the current curve as given by Equations 1 and 2 (Ref. 23).

$$I_pT_p = \int I_p(t)dt \quad (1)$$

$$I_bT_b = \int I_b(t)dt \quad (2)$$

$I_p(t)$ and $I_b(t)$ are the instantaneous values of current at the infinitesimal time duration dt during the pulse cycle. The time interval in this case is the time between

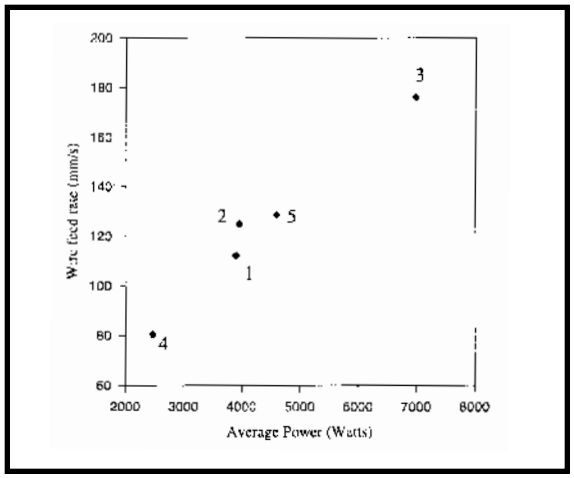

Fig. 4 — Wire feed rate as a function of power input for several sets of pulsing parameters that produce ODPP transfer. Numbers on the points correspond to those on Table 4.

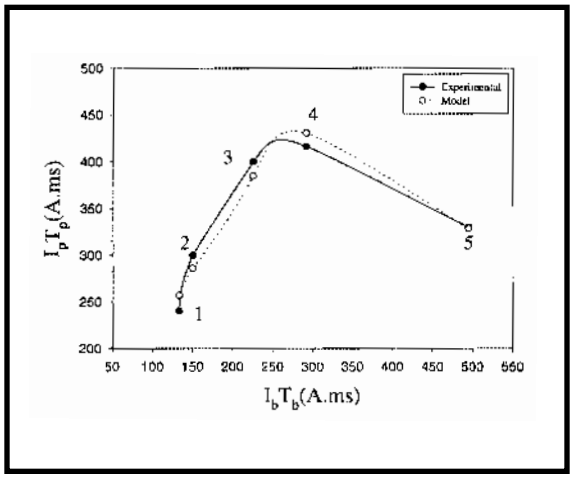

Fig. 5 — Relation between peak and background conditions for ODPP using nominal values of I_p and I_b shown in Table 4.

Table 1 — Parameter Levels for Wire Feed Rate Model

Parameter	Level 1	CP[(a)]	Level 2
Peak current (A)	320	340	360
Background current (A)	70	95	120
Duty cycle (%)	20	27.5	35
Pulsing frequency (Hz)	100	200	300
Tip-to-work distance (mm)	15	20	25

(a) Center point.

Table 2 — Pulse Parameter Range for Identifying ODPP

	Lower limit	Midpoint	Upper limit
Peak current (I_p)	250 A	325 A	400 A
Background current (I_b)	50 A	100 A	150 A
Duty cycle (D)	10%	25%	40%
Pulsing frequency (F)	50 Hz	225 Hz	400 Hz

consecutive sampling points (0.02 ms).

Computing the I_pT_p and I_bT_b values in this way accounts for the effects of power supply behavior such as rise time and overshoot, minimizing the power supply dependence of these results.

Experimental Procedure

To understand the general effect of different parameters on the process and to develop a linear wire feed rate model, a screening experiment was carried out. A two-level fractional factorial experimental design (2^{5-1}) with four center points was performed with the levels shown in Table 1. The design resulted in 20 experimental runs. A commercially available software package was used to set up the design matrix and for fitting a model to the data (Ref. 24).

Bead-on-plate welds were made on a 2.5-mm-thick aluminum plate. For each of the rows of the experimental design matrix, wire feed rate was kept as the response. The wire feed rate was adjusted until the correct value was established. The criteria for establishing the correct wire feed rate were a good stable arc, an approximately constant arc length and average process voltage, and a uniform quality bead. Several test welds for a given experiment might be required to establish a correct output. All the welds were made at a travel speed of 100 in./min. As pulsing conditions varied, uniform beads of different sizes were obtained.

The results of the two-level screening DOE were used as a guideline in designing a three-level D-optimal experimental design with a wider range of parameters. The purpose of the three-level experiment was to determine (Ref. 22) the metal transfer mode and characterize the ODPP regime. The parameter ranges for the three-level DOE are shown in Table 2, and the corresponding design matrix is shown in Table 3. Based on preliminary observations of droplet transfer mode, some runs at peak currents of 300 and 320 A were also added in the design matrix. This is possible in a D-optimal design, which will be discussed later in this paper (Ref. 25).

Methodology and Results

Screening Experiments

As explained in the experimental section, the first step of the methodology consists of performing a two-level design of experiment (DOE) for the five factors, namely peak current (I_p), background current (T_b), duty cycle (D), pulsing frequency (F) and travel speed (S), and their influence on the wire melting rate or wire feed rate (W). The purpose of this experiment is simply to roughly identify a stable operating region in which an arc can be struck and melt-through does not occur. The two-level DOE can also be used to identify the correct gas flow rates, welding gun angles and other fixed factors.

Wire Feed Rate Determination

Clearly, the wire feed rate must match the melting rate for stable operation. Low wire feed causes meltback, and a high feed rate can cause the arc to extinguish through short circuiting. Most wire feed rate models are based on computations of arc and resistance heating of the wire during welding (Ref. 26), using energy principles or experiments. The most common equation used for determining wire feed is based on the equation by Lesnewich (Ref. 27).

$$W = a_a I + b_r LI^2 \quad (3)$$

where W = wire feed rate, L = electrode extension, a_a = factor accounting for localized arc heating at the wire tip, b_r = factor describing resistance heating along wire length.

The constants in this experiment are

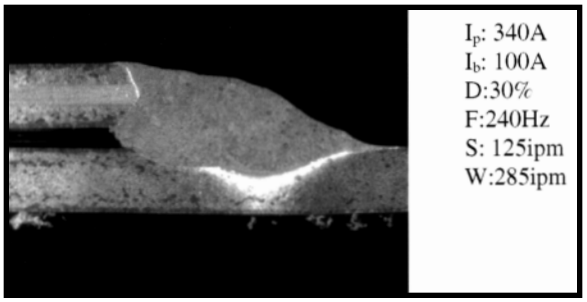

Fig. 6 — Weld bead with procedure resulting in ODPP. Joining of 1.5-mm extrusions.

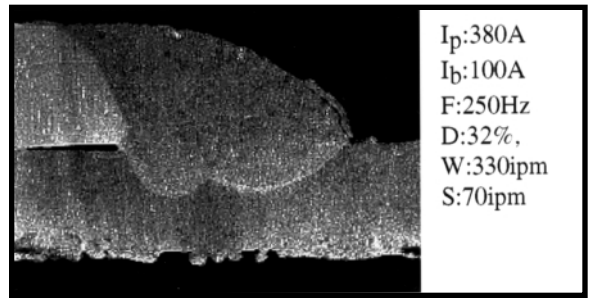

Fig. 7 — Weld bead of 2.5-mm casting to 2-mm extrusion.

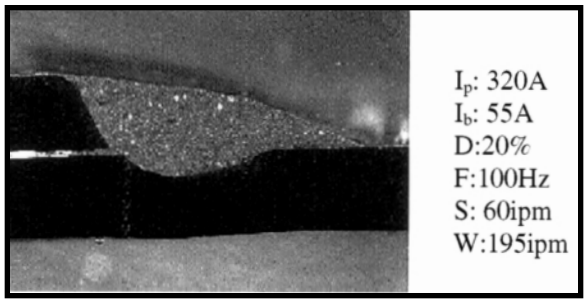

Fig. 8 — Weld bead of 1.5-mm, 1.5-mm lap joint.

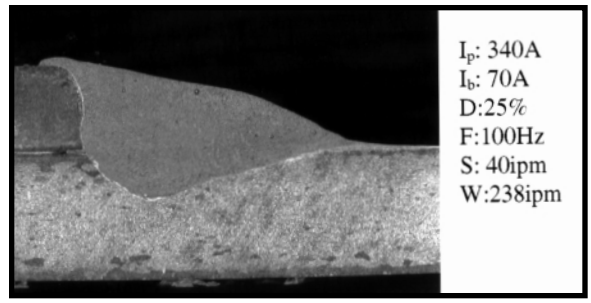

Fig. 9 — Weld bead of 2-mm, 3-mm lap joint.

determined experimentally. For aluminum resistance heating is assumed to be negligible.

This equation has been modified for GMAW-P by integrating over one pulse cycle as (Ref. 28)

$$W(t) = \text{Instantaneous melting rate}$$

$$W = \int_{\text{cycle}} W(t)dt$$

$$\approx (W_p T_p + W_b T_b)F \qquad (4)$$

where W_p = wire melting rates in peak current, W_b = wire melting rate in background current, F = pulse frequency, T_p=peak time, T_b = background time.

This equation is not sufficiently accurate to be used to generate pulsing parameters on an a priori basis for GMAW-P of aluminum over a wide range. The primary reason for this inaccuracy is a failure to account for the effect of pulsing frequency and electrode extension in aluminum, but the model also does not account for power supply dynamics. The actual current values can be quite different from the nominal values in the peak phase. As a result, wire melting during peak and background cannot be simply added assuming a square wave pulse.

The values of wire feed rate obtained in the two-level screening DOE described earlier were used to develop a linear wire feed rate model. The following equation was found to fit the data:

$$W = 0.14*(I_p) + 1.08*(I_b) + 4.18*(D) + 0.03*(F) + 0.8*(L_{tp}) \qquad (5)$$

where I_p = peak current, I_b = background current, D = duty cycle, F = pulsing frequency, L_{tp} = contact tip to plate distance.

Statistical analysis of variance was carried out for these results. The R^2 value was found to be 0.9992, which shows that the model fit the experimental data accurately. The equation shows that the background current and duty cycle are the most significant factors affecting wire feed rate, in the range of parameters studied in the two-level experiment. Though a higher order quadratic equation would show the effect of interactions, it would be more complicated. The linear fit to the experimental data presented here, however, provides a useful tool to quickly establish a wire feed rate for a stable welding operation.

In some parameter ranges, the wire feed rate predicted by Equation 4 and the model presented here can be quite different, as shown in Fig. 2. Figure 2 shows the predicted wire feed rates under the same conditions using Equation 4 and Equation 5 at different pulsing frequencies. This difference could result in an unstable operation.

Once the wire feed rate required for stable operation as a function of the pulsing parameters is determined from the regression analysis, the next step is to identify the pulsing parameters that produce the desired one droplet per pulse (ODPP) transfer over a wide range. To minimize the experimentation needed, D-optimal designs are used, as discussed in the next section.

Metal Transfer Mode Experiments

D-Optimal Designs

The most commonly used experiment designs are cubic in nature and attempt to generate orthogonal data. However, in some applications, irregular experimental regions are found due to physical or economic constraints. This problem is often encountered in attempting to conduct designed experiments on welding processes. It is often impossible to establish an arc, or melt-through may occur under certain experimental conditions needed to satisfy the typical orthogonal experimental design. In these circumstances, the experimenter is forced to either limit the range of the experiment, making it difficult to accurately characterize the entire process space, or to resort to methods of describing "bad data," which cause inaccuracies in the regression anaysis (Refs. 25, 29).

As a result, it is sometimes useful to employ other types of experiment designs to model a process. D-optimal designs offer the flexibility to solve such problems by allowing the experimenter to modify the design space by including and excluding operating points, an im-

Table 3 — Design Matrix for D-Optimal Experiments To Find ODPP

S. No.	I_p A	I_b A	D %	F Hz	W in./min	Observed Transfer
1	400	150	10	50	262	>ODPP
2	400	150	40	400	416	ODPP
3	325	50	10	225	130	<ODPP
4	325	150	10	50	252	>ODPP
5	400	50	25	400	240	<ODPP
6	250	100	10	50	198	>ODPP
7	400	50	10	50	155	>ODPP
8	400	50	40	400	315	>ODPP
9	325	50	25	50	205	>ODPP
10	400	100	10	400	198	>ODPP
11	400	100	40	50	345	>ODPP
12	300	150	10	400	255	<ODPP
13	250	50	10	400	135	<ODPP
14	300	150	40	50	328	>ODPP
15	300	100	40	400	295	ODPP
16	300	150	25	225	304	ODPP
17	250	50	40	50	220	>ODPP
18	320	55	20	150	190	ODPP
19	400	70	25	400	265	ODPP

Table 4 — Pulse Parameters Giving ODPP with Programmed and Measured Values

S.No.	I_p (A)	I_b (A)	D (%)	F (Hz)	T_p (ms)	T_b (ms)	I_pT_p (programmed)	I_bT_b (programmed)	I_pT_p (Actual)	I_bT_b (Actual)	I_{av} (A)	W (in./min)
1	400	70	25	400	0.6	1.9	240	133	276	100	152	265
2	300	100	40	400	1	1.5	300	150	337	120	180	295
3	400	150	40	400	1	1.5	400	225	470	175	250	416
4	320	55	20	150	1.3	5.3	416	291	410	277	108	190
5	300	150	25	225	1.1	3.3	330	495	397	459	187	304

possibility in classical designs. Exclusion of individual runs from the experimental design is generally accomplished by specifying an exclusion formula to remove the infeasible points from the original full factorial candidate set. Inclusions are usually experimental settings for which data already exist prior to the experiment, although inclusion formulas can also be specified, leading to greater experimental efficiency (Refs. 25, 29).

The D-optimal approach also supports smaller three or more level experiments. In a conventional factorial design of experiments, the number of experiments necessary for orthogonal design can become prohibitive as the number of levels increases. For nonlinear processes such as welding, this ability to more efficiently model three or more levels is another important advantage of D-optimal designs. Though calculated effects from D-optimal experimental designs are not perfectly orthogonal/independent, errors are minimized, and this is considered an acceptable trade-off for the flexibility and efficiency gained using D-optimal designs.

In our work, D-optimal experiments were used after the wire feed rate model was established to determine the conditions for one droplet per pulse transfer. The parameter levels of the four pulsing parameters used in this experiment are shown in Table 2. Only 19 experiments at three levels were required to roughly characterize metal transfer behavior using this approach, as shown in Table 3 (Ref. 23).

Mapping of One Droplet Per Pulse (ODPP)

As noted previously, it is generally reported that it is important in GMAW-P to establish pulsing parameters that provide ODPP transfer (Refs. 14–19). The ODPP condition is also reported to result in welds with minimal defects and spatter (Ref. 30). Empirical relations of the form $I_p T_p = C$ have been proposed by previous researchers for work done at low background currents in attempting to characterize the ODPP transfer regime.

By analyzing the high-speed films and voltage signals, experiments that resulted in one drop per pulse were identified for developing an empirical model. Unlike previous efforts, this model takes into account the background conditions (Ref. 23). As the actual values of current and voltage are used, it is a generic model for this wire diameter and composition.

Results of Metal Transfer Experiments

To be consistent with previous work (Refs. 18, 19), the relationship between the peak and background conditions for these experiments was used to characterize the ODPP region as shown in Fig. 3. An equation fitting these points was identified, relating the peak and background conditions by a combination of exponential and Lorentzian function, as given by Equation 6, where T_p and T_b are peak
and background times in ms.

$$I_pT_p = 496.1*\left(1-e^{-0.003*I_bT_b}\right)+\frac{270.1}{\frac{\left(I_bT_b-182.2\right)^2}{8423.5}+1} \quad (6)$$

This equation can be rewritten to find the peak time as a function of the peak current, background current and time as in Equation 7.

$$T_p = \left[496.1*\left(1-e^{-0.003*I_bT_b}\right)+\frac{270.1}{\frac{\left(I_bT_b-182.2\right)^2}{8423.5}+1}\right] / I_p \quad (7)$$

This can be used to define the minimum time at peak required for droplet detachment at a desired peak current level. Table 4 shows the pulsing parameters that result in ODPP. Table 4 also shows the average currents over a fairly wide range of 108–250 A and the corresponding wire feed rates. Depending on the heat input and deposition rates required, a user can start with a particular procedure and use Equation 7 as a tool to find parameters that provide ODPP at a particular average current.

Like the power law approaches used by others (Refs. 18, 19), this equation does not incorporate frequency — the number of droplets transferred in a single pulse, strictly a function of the relationship between time at peak current and peak current values (assuming $I_bt_b << I_pt_p$). Frequency of pulsing will affect deposition rate by controlling the number of times in a given time interval in which these droplets transfer. This Equation 7 provides a simulation tool that can be used to study different pulse parameters before starting any experimental work. It decreases trial and error experimentation required to develop welding procedures and provides a systematic methodology to identify suitable pulse parameters. The peak current and background conditions can be fixed, and the wide range of required peak time can be computed from the equation. Once the peak time is known, the pulsing frequency to obtain ODPP conditions can be calculated.

Selection of Pulsing Parameters

Once the ODPP region has been characterized, it is possible to identify the welding parameters that are most desirable for a given application. Depending on the application, minimizing heat input, maximizing deposition rates or increasing travel speed may be the major concern.

In this work, minimizing heat input to the thin section material and obtaining high productivity were both issues to be addressed. Figure 4 shows the relationship between the power input and wire melting rate during ODPP transfer for this wire. To minimize the heat input, the pulse parameters can be set such that power input to the process is minimized for a particular deposition rate. Figure 4 shows how the melting rate increases with power input, which is again a function of the pulsing parameters. All of the data points represent ODPP transfer conditions using different combinations of pulsing parameters. Between points 2 and 3 (which have different pulsing parameters but the same droplet transfer frequency) the change in power input is only 1.4%, but it results in an increase in deposition rate of about 11%. Looking at points 3 and 4 on the plot, an increase in total power input of about 16% results in an increase in melting rate of only 3%. These results are directly related to the metal transfer behavior, and it is important to understand the influence of all the pulsing parameters when optimizing the process. By allowing one to characterize the range of parameters within which we can obtain ODPP with minimal trial and error experimentation, this work provides an efficient starting point for procedure development.

Modeling Using Programmed Values

The data presented here are based on continuously measured values of I_p and I_b at the weld. Actual, rather than nominal values, are not always available, but this methodology could be applied using the programmed pulse parameters for a particular power supply, as shown here for a Miller Maxtron 450. A plot of the relationships between I_pT_p and I_bT_b for ODPP conditions using programmed values is shown in Fig. 5.

A simple quadratic polynomial is a good approximation to the experimental data, as given by Equation 8.

$$I_pT_p = -0.0044(I_bT_b)^2 + 2.97*(I_bT_b) - 60.13 \quad (8)$$

A comparison of Figs. 3 and 5 illustrates why welding procedures are so machine dependent; actual and nominal values of the critical parameters, peak current and time at peak current, all vary significantly.

Welding Parameter Selection

The model given by Equation 6 is a generic model applicable to any power supply because it is based on the actual heat input delivered to the weld. For a specific power supply, it is easier to develop welding procedures with the model developed from the programmed values, given by Equation 8. The results of the methodology presented here were used to develop welding schedules. These conditions lie close to the curve on Fig. 5. If current values are recorded while welding is carried out, the actual values of I_pT_p and I_bT_b calculated will lie on the curve in Fig. 3. Figure 6 shows the bead geometry of a weld in a lap joint on a 1.5-mm extrusion with ODPP conditions, which met applicable quality requirements for the products of interest in this study ('S' is the travel speed) (Ref. 31). Figure 7 shows welding of an aluminum extrusion to a casting with a procedure resulting in ODPP, with the thinner section at the bottom.

Although ODPP is usually considered to be the ideal in GMAW-P (Ref. 32), in a number of cases, good quality welds were made under conditions of more than one droplet per pulse. Figure 8 shows a weld joining a 1.5-mm extrusion. This welding condition resulted in two drops per pulse. The I_pT_p value for this condition lies above the curve shown in Fig. 5. This shows that the peak conditions in this case were higher than necessary for ODPP, but still produced a good quality weld. Figure 9 shows the weld bead for joining 2–3-mm extrusions. The peak conditions in this case are also higher than needed for ODPP.

Conclusions

A method has been developed that provides an efficient approach for selecting pulsing parameters while requiring considerably less experimentation than conventional approaches. This is a five-step process consisting of screening experiments, development of wire feed rate model, D-optimal experimental design, identification of ODPP region from metal transfer analysis and optimization for a particular application.

Combining a two-level DOE with the D-optimal experimental design provides a way to identify the operating envelope while incorporating the physical constraints of the process to improve experimental efficiency.

Developing a simple linear wire feed rate model reduces trial and error experimentation during pulsing parameter development and helps identify factors to be controlled for maximizing productivity. D-optimal design allows the ODPP region to be characterized using very few experiments.

This methodology can help minimize the power supply dependence of the results by considering actual pulsing conditions. The data needed can be obtained using only an oscilloscope to collect actual current values as a function of time. However, nominal values can also be used. The one droplet per pulse condition can be characterized by detecting droplet detachment in the voltage signals. This technique also provides an efficient way of conducting experiments for process development, allowing any user to rapidly determine viable pulsing schedules.

Acknowledgments

The contributions of William Weber, David Scholl, Richard Allor, Rick Baer and Joe Williams to the experimental work described here are gratefully acknowledged.

References

1. Amin, M. 1981. Synergic pulse MIG welding. *Metal Construction* 13(6): 349–353.

2. Rogers P. 1985. Synergic MIG in perspective. *Metal Construction* 17(9): 602–604.

3. Nacey, T. J. 1993. Fourth generation inverters add artificial intelligence to the control of GMA welding. *Welding Journal* 72(1): 31–34.

4. Salter, G. R., and Doherty, J. 1981. Procedure selection for arc welding. *Metal Construction* 13(9): 544–550.

5. Harris, P., and Smith, B. L. 1983. Factorial techniques for weld quality prediction. *Metal Construction* 15(11): 661–666.

6. Pandey, S., and Parmer, R. S. 1990. Mathematical models for predicting bead geometry and shape relationships for MIG welding of aluminum alloy 5083. *Proceedings of the 2nd International Conference on Trends in Welding Research*, eds. S. A. David and J. M. Vitek, pp. 37–41, ASM International, Materials Park, Ohio.

7. McGlone, J. C. 1982. Weld bead geometry prediction — a review. *Metal Construction* 14(7): 378–384.

8. Thorn, K., Feenstra, M., Young, J. C., Lawson, W. H. S., and Kerr, H. W. 1982. The interaction of process variables — their influence on weld dimensions in GMA welds on steel plate. *Metal Construction* 14(3):128–133.

9. Subramaniam, S., Misra, S., Pandey, S., and Sharma, P. B. 1992. Optimization of weld-

ing procedure for GMAW of aluminum alloy 5083. *Proceedings of the 3rd International Conference on Trends in Welding Research.* eds. S. A. David and J. M. Vitek, pp. 461–466. ASM International, Materials Park, Ohio.

10. Smati, Z. 1986. Automatic pulsed MIG welding. *Metal Construction* 18(1): 38R–44R.

11. Amin, M. 1983. Pulse current parameters for arc stability and controlled metal transfer in arc welding. *Metal Construction* 15(5): 272–277.

12. Needham, J. C. 1965. Pulse controlled consumable electrode welding arcs — general principles and operating characteristics. *British Welding Journal* 4:191–197.

13. Boughton, P., and Lucey, B. A. 1965. The use of pulsed current to control metal transfer in welding. *British Welding Journal* 4: 159–166.

14. Matsuda, F., Ushio, M., and Tanaka, Y. 1983. Metal transfer characteristics in pulsed GMA welding. *Transactions of JWRI* 12(1).

15. Matsuda, F., Ushio, M., Tanaka, Y., Itonaga, K., and Yokoo, T. 1984. Pulsed GMAW: one-drop-transfer and process parameter. *Transactions of JWRI* 13(2): 15–20.

16. Ueguri, S., Hara, K., and Komura, H. 1985. Study of metal transfer in pulsed GMA welding. *Welding Journal* 64(8): 242-s to 250-s.

17. Kim, Y. S., and Eagar, T. 1993. Metal transfer in pulsed current gas metal arc welding. *Welding Journal* 72(7): 279-s to 287-s.

18. Allum, C. J. 1983. MIG welding — time for a reassessment. *Metal Construction.* 15(6): 347–353.

19. Rajasekharan, S., Kulkarni, S. D., Mallya, U. D., and Chaturvedi, R. C. 1995. Molten droplet detachment characteristics in steady and pulsed current GMA welding Al-Mg alloys. *Proc. Sixth Int. Conf. on Aluminum Weldments*, pp. 207–214. American Welding Society, Miami, Fla.

20. Reference Manual. *FORD ACCELL* Welding System, AMET, ID.

21. Allemand, C. D., Schoeder, R., Ries, D. E., and Eagar, T. W. 1985. A method of filming metal transfer in welding arcs. *Welding Journal* 64(1): 45–47.

22. Subramaniam, S., White D. R., Jones, J. E., and Lyons, D. W. 1998. Analysis of arc voltage, current, and light signals in pulsed gas metal arc welding of aluminum. *Science and Technology of Welding and Joining* 3(6):304–311.

23. Subramaniam, S., White, D .R., Jones, J. E., and Lyons, D. W. 1998. Droplet transfer in pulsed gas metal arc welding of aluminum. *Welding Journal* 77(11): 458-s to 464-s.

24. *Statgraphics PLUS*. Ver. 7, Manugistics. 1993.

25. RS/Discover. Statistical Appendices. BBN Software Products Corporation. 3-1:26, 1989.

26. Subramaniam, S. 1996. Wire feed rate model for pulsed gas metal arc welding of aluminum. Winner of Henry Granjon student paper competition. International Institute of Welding.

27. Lesnewich, A. 1958. Control of melting rate and metal transfer in gas-shielded metal arc welding part I — control of electrode melting rate. *Welding Journal* 37(8): 343-s to 353-s.

28. Quintino, L., and Allum, C. J. 1984. Pulsed GMAW: interations between process parameters — part 1. *Welding and Metal Fabrication* 3: 85–89.

29. Snee, R. D. 1985. Computer aided design of experiments — some practical experiences. *Journal of Quality Technology* 17(4): 222–236.

30. Takeuchi, Y., and Shinoda, T. 1991. Spatter and blowhole formation in pulsed gas shielded metal arc welding. *Materials Science and Technology* 7(9):869–876.

31. Subramaniam, S. 1996. Process modeling and analysis for pulsed gas metal arc welding of an aluminum automotive spaceframe. Ph.D. dissertation. Morgantown, W.Va., West Virginia University.

32. Needham, J. C., and Carter, A. W. 1965. Material transfer characteristics with pulsed current. *British Welding Journal* 5: 229–241.

COLOR REPRINTS AVAILABLE

Hydrogen-Induced Cracking along the Fusion Boundary of Dissimilar Metal Welds

BY M.D. ROWE, T. W. NELSON AND J. C. LIPPOLD

Full-color reprints of the subject paper, originally published in the February 1999 *Welding Journal*, are now available at no charge from the AWS Publication Services Division. This reprint includes a full set of color illustrations, as originally submitted by the authors. For a copy, please call the *Welding Journal* offices at (800) 443-9353, Ext. 348, or fax us at (305) 443-7404.